Smoothing and automated picking of kinematic wavefield attributes

Tilman Klüver and Jürgen Mann, Geophysical Institute, University of Karlsruhe, Germany

Summary

Tomographic methods for the determination of velocity models making use of kinematic wavefield attributes strongly depend on the accuracy of these attributes and their efficient extraction from the seismic prestack data. We use the Common-Reflection-Surface (CRS) method to estimate these attributes from the data. Our aim is to improve the quality of the attributes and to extract those values from the CRS output, which are necessary to perform a CRS-based tomography. This extraction should be highly automated and efficient as well as reliable.

Both, smoothing and picking, make use of the same technique: application of locally valid statistics in small windows aligned with the reflection events. We discuss this approach in detail and apply both algorithms to a synthetic 3D dataset. The results clearly show the improved quality of the kinematic wavefield attributes and the stability of the picking process.

Introduction

The Common-Reflection-Surface (CRS) stack method has been developed as an alternative to the conventional normal moveout(NMO)/dip moveout(DMO)/stack procedure. In the last years, interest in the CRS stack parameters itself, the so called kinematic wavefield attributes, has strongly increased. Meanwhile, they are used in a lot of applications: estimation of projected Fresnel-zones, tomographic and Dix-type velocity model determination, minimum aperture Kirchhoff depth migration, etc.

A consistent depth imaging workflow has been set up combining the CRS stack, tomographic velocity model determination, and (true-amplitude) Kirchhoff depth migration (Hertweck et al., 2004). A largely simplified version of this workflow is shown in Figure 1 which is worked through from top to bottom. This workflow has been successfully applied to several 2D and 3D datasets.

The tomographic velocity model determination (Duveneck, 2004) depends on the kinematic wavefield attributes provided by the CRS stack. In order to perform the tomography, the needed attribute values have to be extracted from the CRS results. This should be done in a fast and robust way. Errors in the wavefield attributes due to noise, outliers and statistical fluctuations should be removed before their usage in tomography. For this purpose, Mann and Duveneck (2004) introduced an event-consistent smoothing algorithm for the 2D case, which makes use of small windows aligned with the reflection events. In this paper, the algorithm will be extended to the 3D case where the small window becomes a volume. Such a volume will also be used in a highly automated picking strategy which provides the input for CRS-based tomography.

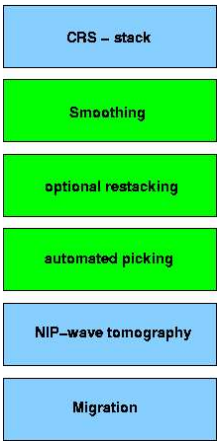

Figure 1: Simplified CRS-based imaging workflow. This paper deals with the boxes highlighted in green.

The combination of small volumes aligned with reflection events and locally valid statistics results in

- an event-consistent smoothing algorithm to remove non-physical fluctuations and outliers from the kinematic wavefield attributes,
- a simple and highly automated picking strategy to extract reliable attribute values from the CRS results.

Basics of CRS stack

The CRS method is based on a second-order approximation of the kinematic reflection response of a reflector segment in depth. In the 3D case, the CRS operator in its hyperbolic form reads

$$t^2(\mathbf{x_m}+\Delta\mathbf{x_m},\mathbf{h}) = \left(t_0^2 + 2\mathbf{p_m}\Delta\mathbf{x_m}\right)^2 + 2t_0\left(\Delta\mathbf{x_m}^T\mathbf{M}_N\Delta\mathbf{x_m} + \mathbf{h}^T\mathbf{M}_{NIP}\mathbf{h}\right). \quad (1)$$

This operator approximates the traveltimes along paraxial rays in the vicinity of a zero-offset (ZO) central ray emerging

at the midpoint location $\mathbf{x_m}$. The ZO two-way traveltime is given by t_0, $\Delta\mathbf{x_m}$ denotes the midpoint dislocation and $\mathbf{h}$ the offset vector. A similar formulation of the 3D CRS operator can be found in Bergler et al. (2002).

The operator (1) depends on a total number of eight attributes: two components of the horizontal slowness vector $\mathbf{p_m}$ and six independent components of the matrices $\mathbf{M}_N$ and $\mathbf{M}_{NIP}$ containing second traveltime derivatives with respect to the midpoint and offset coordinates, respectively. Similar to conventional stacking velocity analysis, these parameters are determined by means of coherence analysis. This results in a 3D volume for each of these parameters.

Assuming the near-surface velocity to be known, these eight stacking parameters can be related to the so-called kinematic wavefield attributes. These are the azimuthal direction α and emergence angle β of the ZO central ray as well as the curvature matrices $\mathbf{K}_\mathrm{N}$ and $\mathbf{K}_\mathrm{NIP}$ of two hypothetical wavefronts related to the so-called normal (N) and normal-incidence-point (NIP) wave (Hubral, 1983).

Basics of CRS-based tomography

A 2D sketch of the normal and NIP-wave is shown in Figure 2. The normal-wavefront is related to the exploding reflector experiment. This experiment is not further explained here, because it is not used in the tomographic inversion. The NIP-wavefront is related to a point source placed on the reflector at the normal-incidence-point of the ZO central ray. The NIP-wavefront reaches the acquisition surface after the one-way traveltime $\tau = t_0/2$ with an emergence angle α and a radius of curvature $R_\mathrm{NIP} = 1/K_\mathrm{NIP}$ (left side of Figure 2). In the 3D case, the relationships between the kinematic wavefield attributes and the eight stacking parameters are given by

$$\mathbf{p_m} = \frac{1}{v_0}\,(\cos\alpha\sin\beta, \sin\alpha\sin\beta)^T\,, \tag{2a}$$

$$\mathbf{M}_\mathrm{N} = \frac{1}{v_0}\mathbf{H}\mathbf{K}_\mathrm{N}\mathbf{H}^T\,, \tag{2b}$$

$$\mathbf{M}_\mathrm{NIP} = \frac{1}{v_0}\mathbf{H}\mathbf{K}_\mathrm{NIP}\mathbf{H}^T\,, \tag{2c}$$

where v_0 denotes the near-surface velocity and $\mathbf{H}$ is a rotation matrix from local ray-centered Cartesian to global Cartesian coordinates.

In CRS-based tomography (Duveneck, 2004), a smooth velocity model is determined by iteratively minimizing the misfit between forward modeled and measured data, that is data extracted from CRS results: τ, $\mathbf{p_m}$, and $\mathbf{M}_\mathrm{NIP}$. Descriptively, this means, that a velocity model is searched for, wherein all NIP-waves focus at their correct depth position if propagated back into the subsurface. A similar strategy has been followed by Lavaud et al. (2004), who estimate finite-offset ray emergence angles from the ZO attributes determined by means of the 2D CRS stack.

The aligned window

The basis for both algorithms, smoothing and automated picking, is a small window aligned with the reflection event in the ZO stacked data volume. Inside this window, locally valid statistics can be applied to the kinematic wavefield attributes, coherence values, and stacked amplitudes. In time direction, the window should not be larger than the wavelet of the considered event in order not to mix valuable information with noise or information related to other coherent events. In the spatial directions, the window should not exceed the first projected Fresnel zone. In order to stay inside the considered reflection event, the window is tilted according to the dip of the reflection event in the stacked volume. The dip is given by twice the horizontal slowness vector $\mathbf{p_m}$ as one can see from equation (1).

Using equation (2a), one can easily determine the unit normal vector to the N- and NIP-wavefront:

$$\mathbf{n} = (\cos\alpha\sin\beta, \sin\alpha\sin\beta, \cos\beta)^T\,. \tag{3}$$

Inside an aligned window, this can be done for each sample. This way, the dip difference θ between wavefront normal vectors calculated from different samples is defined as

$$\theta = \arccos(\mathbf{n}_1 \cdot \mathbf{n}_2)\,. \tag{4}$$

Event-consistent smoothing

During the CRS stack, the optimum stacking operator is determined independently for each sample in the ZO volume. In this way, the NMO stretch effect is avoided (Mann and Höcht, 2003). However, the sample-by-sample determination of the stacking parameters might lead to non-physical fluctuations of the attributes in the obtained kinematic wavefield attribute volumes. Due to several facts, a stable determination of attributes might not be possible for every ZO location. In order not to distort further processing steps and results based on these attributes, it is necessary to remove these unwanted fluctuations.

In contrast to v_stack determined in conventional stacking velocity analysis, the spatial traveltime derivatives used to parameterize the CRS stacking operator (1) remain locally constant along the wavelet. Additionally, as long as paraxial ray theory is applicable, these spatial traveltime derivatives should vary smoothly along a reflection event. The application of event-consistent smoothing of the kinematic wavefield attributes is justified on the basis of these two observations. The originally proposed smoothing algorithm for the 2D case (Mann and Duveneck, 2004) can naturally be extended to the 3D case:

For each zero offset sample and CRS parameter

- align smoothing window with the reflection event using first traveltime derivatives
- inside this window, reject samples below user-defined coherence threshold
- reject samples with dip difference θ beyond a user-defined threshold with respect to the central sample
- apply a combined filter:
  - median filter to remove outliers
  - averaging around the median to remove fluctuations
- assign the result to the corresponding ZO central sample

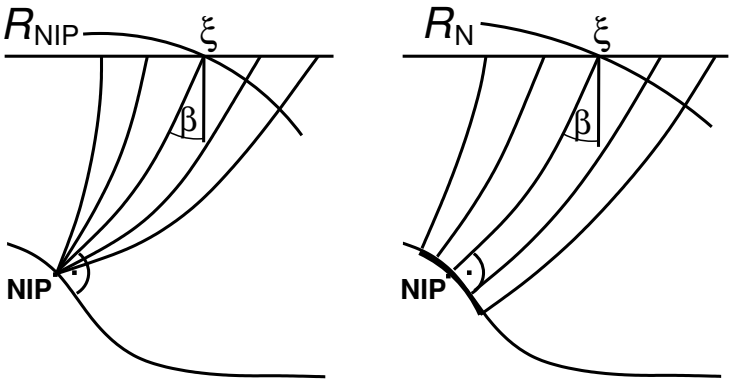

Figure 2: NIP- and normal wave experiment for the 2D case. The normal-incidence-point (NIP) specifies the location where the ZO central ray hits the reflector normally. In the NIP-wave experiment, a point source is placed there. The emerging wavefront due to this experiment has the radius of curvature R_{NIP} at the emergence location ξ of the ZO central ray. In the N-wave experiment, an exploding reflector segment yields a radius of curvature R_N. In both experiments, the ZO central ray has an emergence angle β.

For each smoothed attribute value, only samples on the same reflection event are considered. There is no mixing of intersecting events. This means that conflicting dip situations can be considered in a natural way and do not lead to wrong results. The combination of a mean and median filter turned out to be a simple and robust strategy to remove outliers and fluctuations from the kinematic wavefield attribute volumes.

Automated picking

Having smoothed the kinematic wavefield attributes, they are well suited to be used in the tomographic determination of velocity models. In order to distinguish between valuable information and noise, we apply a coherence-based automatic picking strategy. The coherence gives a direct measure of the reliability of the kinematic wavefield attributes. In other words, the coherence is a direct measure how well the operator (1) fits the prestack data.

However, only using coherence as a reliability criterion in selecting picks can be misleading. as one might also select picks related to noise, which can have quite high coherence values. Therefore, we consider additional criteria. Our automated picking algorithm is formulated in the following way:

For each trace:

- search the coherence maximum on the selected trace and go to the nearest maximum of the stack envelope
- align a window with the reflection event using first traveltime derivatives
- check if a user-defined percentage of all samples inside the window
  - has coherence values higher than a given threshold
  - has a dip difference θ below a given threshold with respect to the central sample
- optionally, check if the amplitude exceeds a user-defined threshold
- continue on the selected trace until a user-defined maximum number of picks on this trace is reached

Valid picks are not only selected according to their coherence value. Additionally, information from neighboring samples on the same reflection event is taken into account. This allows to check if the pick location under consideration is actually part of a locally coherent reflection event.

Synthetic data example

To illustrate the applicability and efficiency of the proposed smoothing and picking strategies, we use a synthetic 3D data example. The considered ZO volume consists of 241 lines with 241 CMP locations each. The line and midpoint spacing is 12.5 m. Each trace in the stacked volume consists of 375 samples with a sampling interval of 8 ms. The prestack data were forward modeled using a wavefront construction technique and, subsequently, the CRS stack was performed. In Figure 3, one inline, one crossline, and one timeslice of the CRS stacked ZO volume is depicted. Displayed on the inline section is the stack itself, on the crossline section the coherence value, and on the timeslice the stacking velocity in inline direction calculated from the kinematic wavefield attributes. In Figure 4, the corresponding sections after smoothing the traveltime derivatives of operator (1) are shown. A comparison shows, that the image quality and lateral continuity of the stack and attribute sections has considerably improved. Based on these smoothed attributes and restacked ZO volumes, we applied our automated picking strategy. In Figure 5, you see the valid pick locations highlighted in green on two inline and one crossline section of the smooth stack volume. All picks are well aligned with the event. There is almost no picking of different phases of the wavelet on neighboring traces, although picking is performed on each trace individually. This is due to considering the envelope of the stack. In some regions, our method did not accept some samples on the event as valid pick locations due to the consideration of neighboring information inside the used aligned window.

All selected pick locations can now be used as input for the tomographic inversion. However, in practice we do not need to use such a high number of picks. Therefore, it is usually not necessary to perform the picking on every trace.

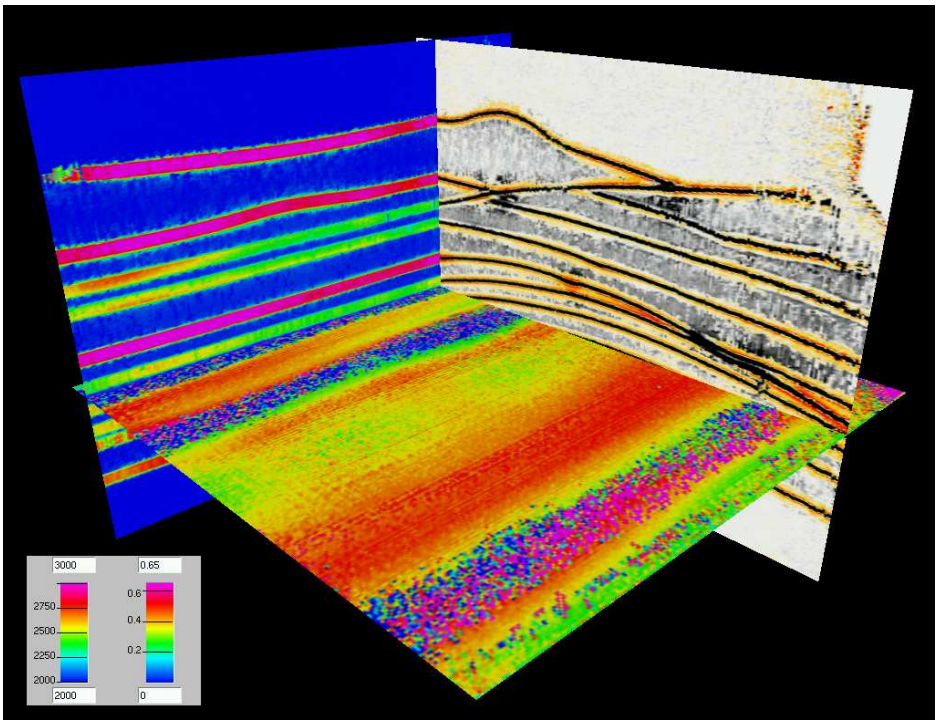

Figure 3: CRS results with unsmoothed kinematic wavefield attributes. A stack section is shown in inline direction, in crossline direction the coherence is shown. On the timeslice, the stacking velocity in inline direction is depicted. The left scale corresponds to stacking velocity in m/s, the right one to the coherence (semblance).

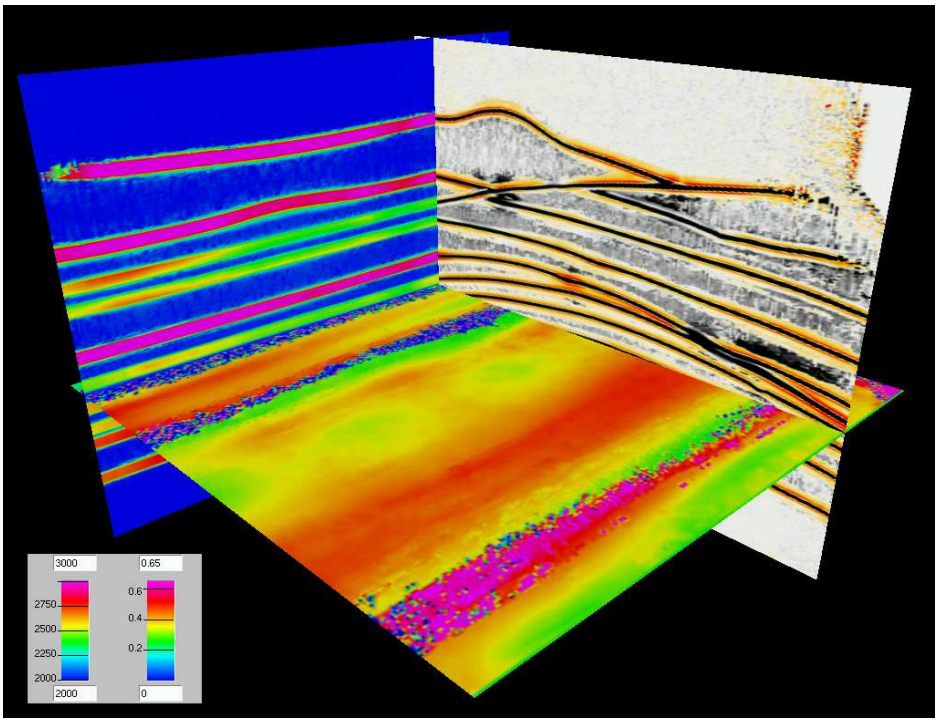

Figure 4: Smoothed kinematic wavefield attributes and CRS results after restacking. In inline direction the restacked section is shown. In crossline the coherence obtained using smoothed attributes is shown. On the timeslice the stacking velocity calculated from smoothed attributes is depicted. The left scale corresponds to stacking velocity in m/s, the right one to the coherence (semblance).

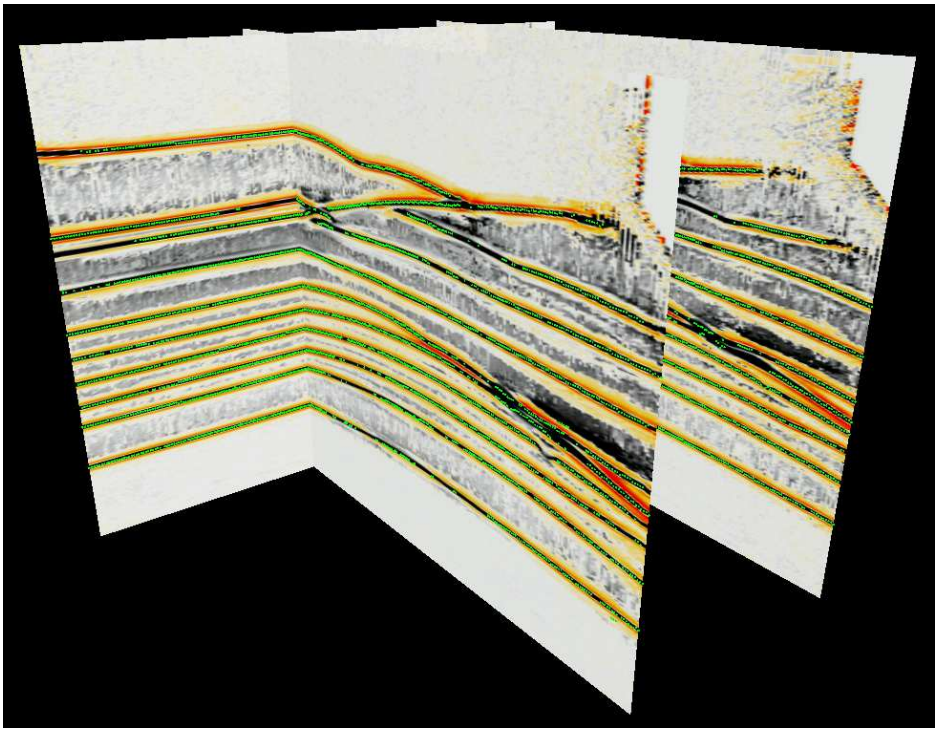

Figure 5: Two inline and one crossline section of the stack obtained using smoothed kinematic wavefield attributes. Valid pick locations are highlighted in green.

Conclusions

We have presented an event consistent smoothing and highly automated picking strategy for CRS wavefield attributes. Both algorithms use locally valid statistics applied in small windows aligned with the reflection events. The smoothing removes outliers and unwanted fluctuations from the kinematic wavefield attributes in a physically sound way. The automated picking strategy extracts these smoothed attributes from the CRS output with minimum human intervention. This is very attractive in the here presented 3D case, where manual picking is a very time consuming and difficult task. These tools are an important contribution to a CRS-based imaging workflow (Hertweck et al., 2004), as they close, in some sense, a gap between the application of the CRS stack and the subsequent usage of CRS attributes.

Acknowledgments

We would like to thank the sponsors of the Wave Inversion Technology (WIT) Consortium for their support.

References

Bergler, S., Hubral, P., Marchetti, P., Cristini, A., and Cardone, G. (2002). 3D Common-Reflection-Surface stack and kinematic wavefield attributes. *The Leading Edge*, 21(10):1010–1015.

Duveneck, E. (2004). Velocity model estimation with data-derived wavefront attributes. *Geophysics*, 69(1):265–274.

Hertweck, T., Jäger, C., Mann, J., Duveneck, E., and Heilmann, Z. (2004). A seismic reflection imaging workflow based on the Common-Reflection-Surface (CRS) stack: theoretical background and case study. In *Expanded Abstracts, 74th Ann. Internat. Mtg.* Soc. Expl. Geophys.

Hubral, P. (1983). Computing true amplitude reflections in a laterally inhomogeneous earth. *Geophysics*, 48(8):1051–1062.

Lavaud, B., Baina, R., and Landa, E. (2004). Poststack Stereotomography – A Robust Strategy for Velocity Model Estimation. In *Extended abstracts, 66th Conf.* Eur. Assn. Geosci. Eng. Session C022.

Mann, J. and Duveneck, E. (2004). Event-consistent smoothing in generalized high-density velocity analysis. In *Expanded Abstracts, 74th Ann. Internat. Mtg.* Soc. Expl. Geophys. Session ST 1.1.

Mann, J. and Höcht, G. (2003). Pulse stretch effects in the context of data-driven imaging methods. In *Extended abstracts, 65th Conf.* Eur. Assn. Geosci. Eng. Session P007.